14th Australasian Fluid Mechanics Conference
Adelaide University, Adelaide, Australia
10-14 December 2001

Interaction between Turbulence Wedges which Develop from Roughness Row in a Flat Plate Laminar Boundary Layer

M. Ichimiya and C. Sudo

Department of Mechanical Engineering
University of Tokushima, Tokushima, 770-8506 JAPAN

Abstract

Experiments were performed to investigate the effect of a three-dimensional roughness row on boundary-layer transitions on a flat-plate with zero pressure gradient. Each roughness element was a cylinder 2 mm in both diameter and height. Eleven elements formed a row in the spanwise direction. Wedge-shaped turbulent regions ("turbulence wedges") developed downstream from the respective roughnesses. Further downstream, two adjacent wedges merged together and then a two-dimensional turbulent boundary layer was formed. Velocities were measured by hot-wire anemometers inside and outside the wedge regions, and an intermittency factor and vorticities for streamwise vortices were obtained.

When we compare the respective turbulence wedges from the present roughness row with a wedge developed from a single roughness element in a previous study, we find that (1) the wedge expansion angle in the spanwise direction with the roughness row was same as that with the single roughness; also wedge developments in the wall-normal direction for both cases were same, (2) more streamwise vortices appeared within the present wedges, (3) the scales of the streamwise vortices in the present wedges were smaller, and (4) the mean vorticities in the present wedges were larger.

Introduction

The laminar-turbulent transition of boundary layers has been investigated for many years. Among these investigations, artificial transitions due to a roughness element have also been investigated [3]. A wedge-shaped turbulent region, or "turbulence wedge," is formed downstream of a single three-dimensional roughness element. The present authors showed in previous studies that just behind the roughness element there were many streamwise vortices; on the other hand, further downstream a pair of streamwise vortices were found on both interfaces between the wedge and the outer laminar region [4,5].

In practice, however, multiple roughnesses are found. Using multiple roughnesses, Gibbings et al. [2] showed start and end points of the transition; however, the way in which the structures in the turbulence wedge are affected by an encounter and interaction between wedges has not been clarified. The present study aims to investigate the transition processes due to a spanwise roughness row, which consists of three-dimensional roughnesses. In particular, this investigation examined whether multiple turbulence wedges downstream of the multiple roughnesses can be regarded as a superposition of many single wedges, the process until a turbulence wedge encounters and interacts with an adjacent wedge, and how the streamwise vortices are affected by the interactions of the wedges.

Experimental Apparatus and Measurement Methods

The experimental setup consisted of a 15 mm thick, 400 mm wide, and 2.0 m long Bakelite plate with a sharpened leading edge mounted horizontally in an open circuit blowing-type wind tunnel. The test section was 400×150 mm in cross section and 2 m in length with a contraction ratio of 10 and a turbulence level of 0.2% at a nominal wind speed of 7.5 m/s. Tani et al. [7] showed that the turbulence intensity does not affect the condition of a transition induced from the roughness position. A wall opposite the working side of the plate permitted adjustments of the zero pressure gradient. The velocity profile near the leading edge was of the Blasius type. The experiment was conducted for the constant unit Reynolds number U_m / ν = 5×10^5 m^{-1}. The reference main flow velocity at the leading edge U_m was about 7.5 m/s.

Figure 1 shows the coordinate system and turbulence wedges. Each roughness element was a cylinder 2 mm in both diameter d and height k. Eleven elements formed a row in the spanwise direction at 100 mm downstream from the leading edge of the flat plate. The clearance between roughnesses, s, was 22 mm, i.e., s/d equaled 11. A turbulence wedge was formed downstream of the respective roughness. Since the boundary layer at this position without the roughness element was laminar with a thickness of about 2.2 mm, the height of the roughness element k was nearly equal to the boundary layer thickness. The roughness Reynolds number based on k and velocity at $y = k$ was 996, thus satisfying the condition under which the turbulence wedge develops from the roughness [6,7]. Here we employ normalized coordinates, X (= $(x-x_k) / k$), Y (= y / k) and Z (= z / d) (x_k is the x position of the roughness, 100 mm).

V- and X-shaped hot-wire probes with two tungsten sensing elements each 5 μm in diameter and 1 mm wide were used in the measurements. The output voltage from the hot-wire was digitized at a 5-kHz sampling frequency during an approximately 20-second sampling period. The velocity distributions were so symmetric with respect to the center of the each roughness element that the experimental results will be shown in a half-pitch region between roughnesses ($0 \leqq Z \leqq 6$).

Results and Discussion

To visualize the spanwise development of a turbulence wedge which was produced by a roughness element, positions where an intermittency factor γ equals 0.5 on a X-Z plane are shown in

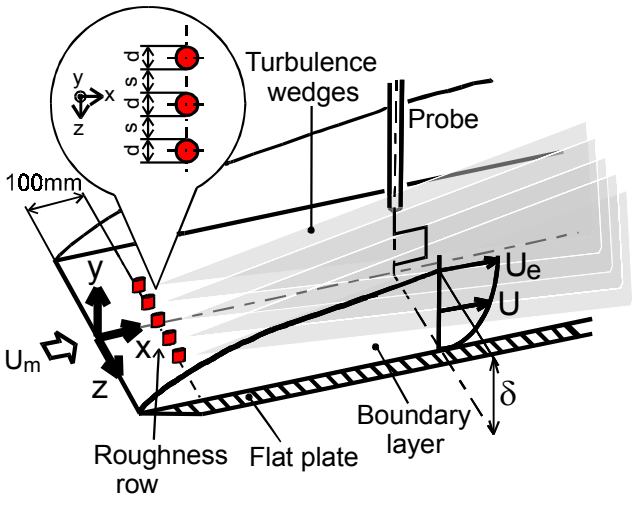

Figure 1. Coordinate system and turbulence wedges.

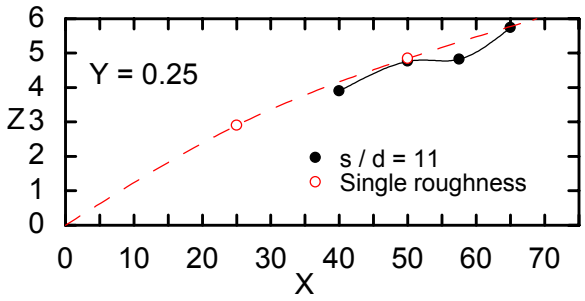

Figure 2. Lateral expansion of the turbulence wedge.

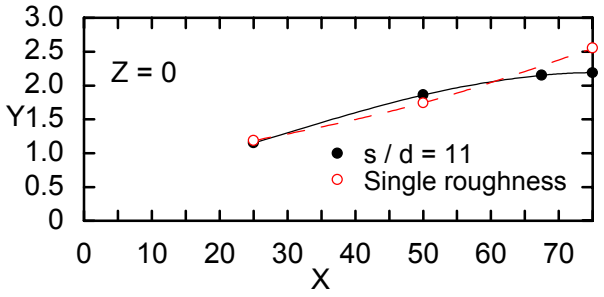

Figure 3. Wall-normal development of the turbulence wedge.

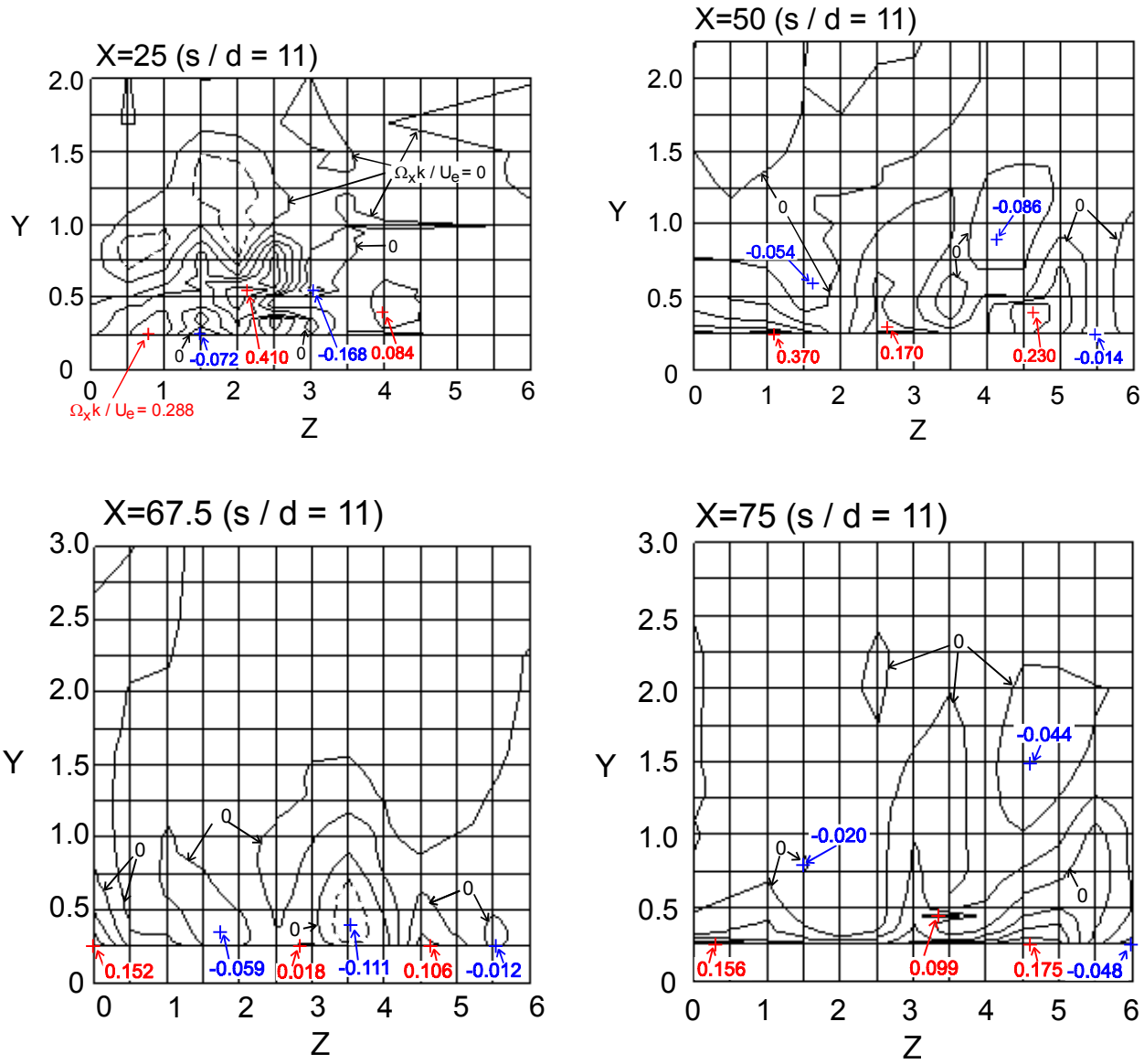

Figure 4. Contour map and maximum values of the mean streamwise vorticity of the roughness row. The solid and broken lines indicate positive and negative values, respectively. Line interval is 0.08. The red and blue crosses indicate positive and negative maximum positions, respectively.

Figure 2. These points correspond to the shape of the wedge. The closed and open circles indicate the wedge from the roughness row s/d = 11 and single roughness [4], respectively. If a time average is done, the wedge is seen to encounter the adjacent wedge at approximately X = 67.5. The spanwise expansions for the roughness row s/d = 11 and the single roughness are almost the same.

Figure 3 shows the wall-normal positions of half-intermittency for two kinds of wedges. The two developments are also almost same.

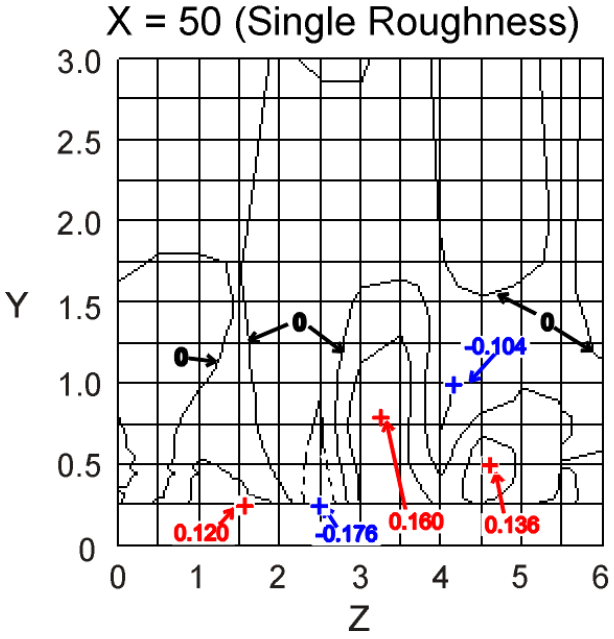

Figure 5. Contour map and maximum values of the mean streamwise vorticity of the single roughness. Line interval is 0.08.

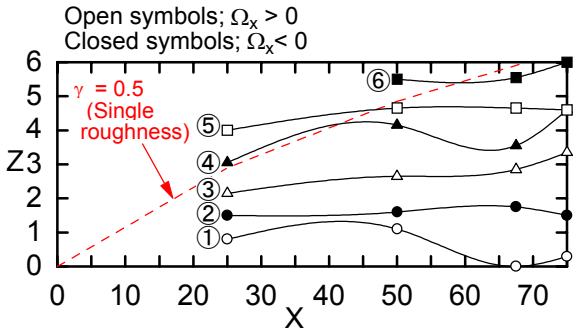

Figure 6. Positions of the vortex centers.

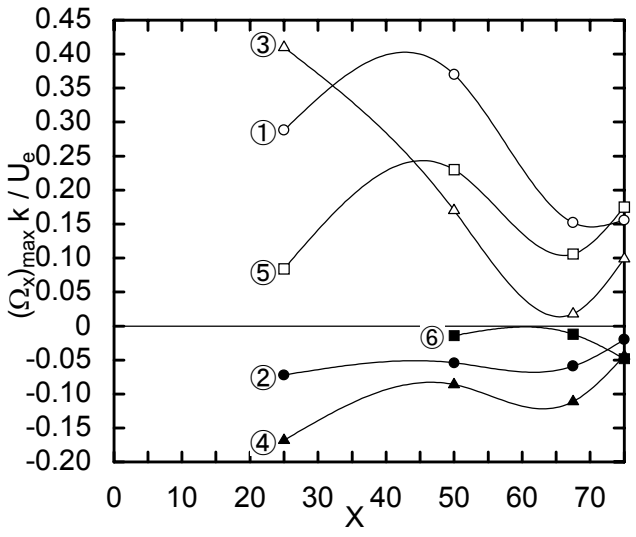

Figure 7. Streamwise variation of the maximum vorticity.

Figure 4 shows contour maps of mean streamwise vorticities $\Omega_x = \partial W/\partial y - \partial V/\partial z$ normalized by the roughness height k and the free stream velocity U_e. For all four streamwise stations, the adjacent streamwise vortices rotate in the opposite direction. The number of vortices increases from five at $X = 25$ to six at $X = 50$. Figure 5 shows a contour map for the single roughness element at $X = 50$. The number of streamwise vortices is five, which is fewer than with the roughness row.

Figure 6 shows the positions of the vortex centers defined as the vorticity maximum positions. The spanwise positions at any streamwise station are almost the same, thus the vortex axes are not oblique like the wedge interfaces but almost parallel to the wedge centerline. de Bruin [1] showed the same result regarding a single roughness element.

Figure 7 shows the streamwise variation of the maximum vorticity. The four inner vortices may be caused directly by the roughness, i.e., the horseshoe, trailing [3] and shedding vortices, etc., and have already induced vortices corresponding to the wedge expansion further upstream than $X = 25$. The absolute values of the vorticities of the vortices within the wedge decrease during the course from $X = 25$ toward $X = 50$ except for that of the innermost vortex. The vorticity of the fifth vortex, on the other hand, which is outside of the wedge at $X = 25$, increases during the same course. At the station, $X = 50$, the new sixth vortex has appeared outside of the wedge. That is, in a streamwise station, the vorticity of the outermost vortex increases until a new vortex originates at an outer spanwise position downstream, while those of the inner vortices decrease in the downstream direction. In the course from $X = 67.5$ to 75, however, vorticities for the fifth and sixth vortices increase. This means that the vorticities of the outer vortices increase due to the encounter and interaction of two wedges.

Table 1 shows a comparison of the maximum vorticities of the respective vortices with the roughness row and the single roughness at $X = 50$. The ratios of the vorticities are larger or smaller than unity in the positive or negative vortices, respectively.

In Table 2, a comparison of the vortex scales, i.e., the area of half-maximum value, is shown. In general, scales with the roughness row are smaller than those with the single roughness.

Vortex number from centerline	$(\Omega_x)_{max}\ k/U_e$ (s/d=11)	$(\Omega_x)_{max}\ k/U_e$ (Single roughness)	Ratio (s/d=11) /(Single)
①	0.370	0.120	3.08
②	-0.054	-0.176	0.31
③	0.170	0.160	1.06
④	-0.086	-0.104	0.83
⑤	0.230	0.136	1.69
⑥	-0.014		

Table 1. Maximum value of mean streamwise vorticity at $X = 50$.

Vortex number from centerline	Scale [mm^2] (s/d=11)	Scale [mm^2] (Single roughness)	Ratio (s/d=11) /(Single)
①	0.16	1.04	0.15
②	2.32	1.23	1.90
③	2.04	2.73	0.75
④	1.40	1.37	1.02
⑤	1.25	1.07	1.17
⑥	0.02		

Table 2. Scale of streamwise vorticities at $X = 50$.

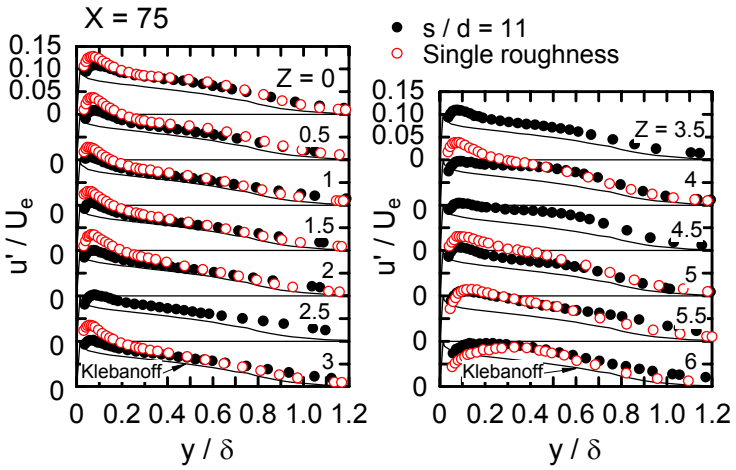

Figure 8. Distributions of the fluctuating velocity component in the streamwise direction at $X = 75$ for Z varying from 0 to 6. Single roughness + s/d =11 data are shown.

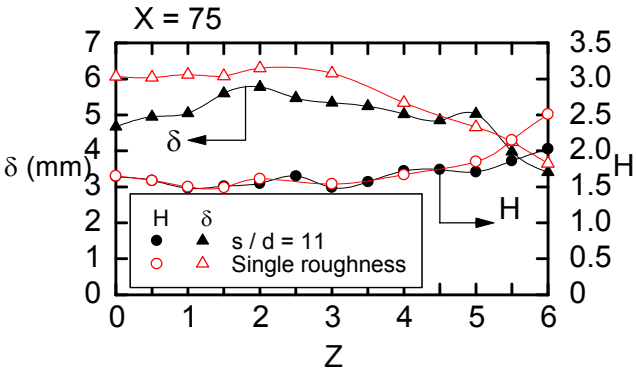

Figure 9. Spanwise distribution of the shape factor and boundary layer thickness at $X = 75$.

As mentioned above, there are five vortices for the single roughness, and six vortices for the roughness row. The wedge expansions in the spanwise and wall-normal directions, however, are almost same in both cases. This suggests that with the roughness row more vortices are packed so much more densely in the spanwise direction than with the single roughness that the scales of the respective vortices will decrease and the vorticities will increase.

Figure 8 shows the wall-normal distribution of the fluctuating velocity component in the streamwise direction u'/U_e with the roughness row and single roughness at $X = 75$. Since this streamwise station is slightly downstream from where two wedges encounter each other, the effects of wedge interaction appear in the distribution at $Z = 5.5$ and 6. That is, the fluctuating velocities with the roughness row are larger than those with the single roughness at these locations.

The turbulence tendency due to the interaction can be seen from the shape factor H at $X = 75$ in Fig. 9. The shape factor with the roughness row is smaller than that with the single roughness at $Z = 5.5$ and 6. That is, the mean velocity profile with the roughness row is closer to the turbulent-type. This means that turbulence is promoted by the encounter and interaction of two wedges. Figure 9 also shows the boundary layer thickness δ. The thicknesses are almost same for both cases at $Z = 5.5$ and 6. On the other hand, the boundary layer is thinner with the roughness row, in the inner region of the wedge. This may be due to the fact that the scale of the vortices is smaller with the roughness row. As can be seen, when two wedges encounter each other the boundary layer thickness does not become simply an addition of the respective thicknesses. Moreover, the boundary layer is thinner than the original value.

Conclusions

Experiments were performed to investigate the effect of a three-dimensional roughness row on boundary-layer transition on a flat-plate with zero pressure gradient. The following conclusions were obtained.

(1) The turbulence wedge expansion angle in the spanwise direction and its developments in the wall-normal direction with the roughness row were the same as with the single roughness.

(2) More streamwise vortices appeared in the turbulence wedge with the roughness row.

(3) The scales of the streamwise vortices were smaller, so the boundary layer was thinner with the roughness row.

(4) The mean vorticities with the roughness row were larger than those with the single roughness.

(5) Due to the interaction of two wedges, the turbulence increased and a turbulent tendency was promoted. The vorticities increased in such locations.

(6) The streamwise vortices exist in almost the same spanwise positions at any streamwise station. The vorticity of the outermost vortex increased until a new outer vortex appeared downstream, and vorticities of the inner vortices decreased in the downstream direction.

References

[1] de Bruin, A.C., The Effect of a Single Cylindrical Roughness Element on Boundary Layer Transition in a Favourable Pressure Gradient, in *Laminar-Turbulent Transition IUTAM Symp. Toulouse/France 1989*, editors D. Arnal & R. Michel, Springer-Verlag, 1990, 645-655.

[2] Gibbings, J.C., Goksel, O.T. & Hall. D.J., The Influence of Roughness Trips upon Boundary-Layer Transition, Part 3. Characteristics of Rows of Spherical Transition Trips, *Aeron. J.*, 90-900, 1986, 393-398.

[3] Gregory, M.A. & Walker, W.S., The Effect on Transition of Isolated Surface Excrescences in the Boundary Layer, *ARC R. & M.*, 2779, 1951.

[4] Ichimiya, M., Nakase, Y. and Fukutomi, J., Structure of a Turbulence Wedge Developed from a Single Roughness Element on a Flat Plate, in *Engineering Turbulence Modelling and Experiments 2*, editors W. Rodi and F. Martelli, Elsevier, 1993, 613-622.

[5] Ichimiya, M., The Effect of a Single Roughness Element on a Flat Plate Boundary Layer Transition, in *Engineering Turbulence Modelling and Experiments 4*, editors W. Rodi and D. Laurence, Elsevier, 1999, 597-606.

[6] Mochizuki, M., Smoke Observation on Boundary Layer Transition Caused by a Spherical Roughness Element, *J. Phys. Soc. Jpn.*, 16-5, 1961, 995-1008.

[7] Tani, I., Komoda, H., Komatsu, Y. & Iuchi, M., Boundary-Layer Transition by Isolated Roughness, *Aeron. Res. Inst. Univ. Tokyo Rep.*, 375, 1962, 129-143.